Study of two-dimensional photonic crystal microcavities filled with polymer

To cite this article: A Benmerkhi *et al* 2010 *IOP Conf. Ser.: Mater. Sci. Eng.* **15** 012094

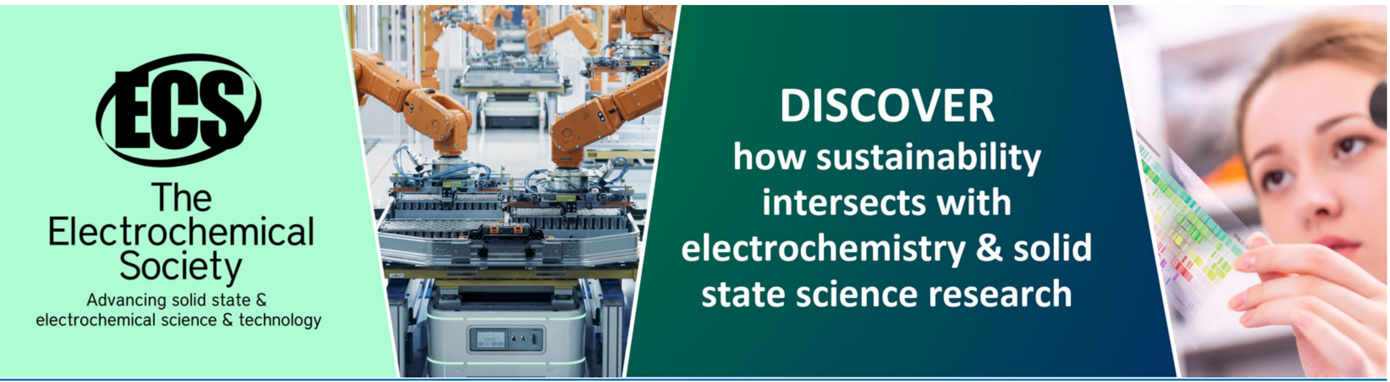

Study of two-dimensional photonic crystal microcavities filled with polymer

A Benmerkhi[1], M Bouchemat[1], T Bouchemat[1] and N Paraire[2]

[1] Electronics department, Mentouri University of Constantine, Algeria.
[2] IEF de Paris Sud, Orsay France

Email: hm_Bouchemat@yahoo.fr

Abstract. We present numerical study of microcavity biosensor in photonic crystal (PC) with triangular lattice of air holes patterned perpendicularly to an InP-based confining heterostructure. The microcavity is formed by varying the radius of one air hole. The 2D finite difference time domain (FDTD) method algorithm (fullwave simulator) is used to compute the light transmission efficiency and the quality factor (Q) when the refractive index (RI) filled in the air holes of water and polymer. The detected spectrum has a Lorentzian line shape, and the peak occurs when the PC cavity is at resonance. The resonance wavelength of this cavity will shift accordingly due to the variation of RI. The polymer filling of photonic crystal holes can be used to measure gas, fluids, biolayers, or bound chemical.

1. Introduction

Photonic crystals (PCs) are artificial materials consisting of a periodic arrangement of low- and high-dielectric materials in one, two, or three dimensions that provide control of light at a wavelength scale [1]. Photonic crystal devices with 1-D, 2-D and 3-D structures have been fabricated by wet dry etching, wafer bonding, self-assembled method and electron-beam lithography [2]. Among these 3-type structures, 2-D photonic crystals can be exploited to realize microcavity lasers and linear waveguides to direct the electromagnetic wave towards specific regions, thus allowing high integration in planar photonic crystal integrated circuits [3, 4]. Among the available materials for photonic applications, such as InP, GaAs, SOI and polymers, the polymers have attracted a great interest, due to their low temperature fabrication, good mass production possibilities with low processing cost, easy functionalization and possibility to tune their optical properties [5, 6]. The functionality of PC structures will increase when their optical properties are tunable. An attractive possibility in this respect is to replace the low-index part (air) with a material that has a tunable refractive index. The infiltration of PC with fluids or polymers for realizing tunable optical devices or sensors was first suggested a decade ago [7] and experimentally demonstrated in both three-dimensional [8] and 2D [9–10] geometries. Optical sensor elements for refractive index (RI) measurements have been subject to research interest, and still today new technologies [11] are suggested. The potential of PC infiltration with organic materials (e.g., liquid crystals or polymers) is thus amplified provided that a selective filling procedure is available. However, only a few examples of locally modified PCs have been published so far [12–13]. Intonti et al. [12] have demonstrated microinfiltration of liquids in a macroporous silicon PC via hollow submicrometer size pipettes and have suggested the possibility of nanoinfiltration with smaller microtips and UV imaging. Smith et al.

[14] have used a similar technique to create a PC double heterostructure based on the theoretical calculations by Tomljenovic-Hanic et al. [15]. Erickson et al. [16] have used nanofluidic targeting to infiltrate a single row of holes within a planar PC using fluids with different refractive indices. Kichen et al. [17] present a novel lithographic technique of tuning PC devices, based on local mask opening for individual holes. This enables the use of any post production method on the exposed area of the PC, while not affecting other holes in the PC. None of the other techniques is capable of being both local on the single hole level and free, regarding the choice of post processing technique. The process is demonstrated by application of both local digital etching and local LC infiltration of the nearest-neighbour-holes of a point defect (H_1) cavity in the technologically important InP system [18].

The application of RI sensors is interesting for both gaseous and aqueous samples and includes measurement of parameters like temperature, humidity, chemical composition and biosensing. The application of RI sensors for biosensing has especially gained a high degree of interest within the last two decades. It includes detection of DNA, proteins, antibody-antigen interactions, cells and bacteria.
Optical microcavities have numerous applications, spanning engineering and science disciplines from designing high-performance optical buffers to studying quantum effects. Recently, these devices have begun to probe biological phenomena, behaving as sensitive and specific chemical and biological sensors. The sensitivity is derived from the long photon lifetime inside the cavity, and therefore, devices with higher quality factors (Q) are more sensitive.

In this paper we demonstrate the photonic band edge shift for a deeply etched 2D PC by filling the air holes with water (n=1.33) and polymer PMMA (polythylmethacrylate) with refractive index n=1.54. We propose a microcavity in 2D PC with triangular lattice of air holes filled with water and polymer; we clearly observe the resonance peak of this cavity redshift. After this study we simulate this cavity locally filled with the same polymer and noticed that the PC size is optimized as 19 x19 air holes to ensure high transmission efficiency and Q factor.

2. The photonic crystal design

In the designed structure shown in Figure 1a, a 2D triangular photonic crystal of air holes patterned perpendicularly to a InP- based confining heterostructure with the effective RI n=3.32 (ε=11) is selected. The lattice constant is a=440nm while the hole radius is r=0.36a. High aspect ratio etching of the photonic crystal is achieved using Ar/Cl_2-based chemically assisted ion beam etching. Details on the sample fabrication are given in [19, 20].

The computational method used is based on a 2D finite difference time domain (FDTD) method algorithm. Perfectly matched layers (PML) conditions have been considered in the calculations to ensure no back reflection in the limit of the analyzed region [21]. This crystal is light by a Gaussian wave under normal incidence with a transverse electric (TM) polarized. The length of the photonic crystal is 13a and the time step is chosen to 0.01. Note that it might be necessary to reduce the time step below the stability limit when simulating metals since the courant condition can change in this case.

Dispersion diagram showing normalized frequency versus the wave vector for TE and TM modes of the 2D photonic crystal is given in figure1b. It has been calculated along the $\Gamma - K - M - \Gamma$ edge for the Brillouin zone by employing a 2D plane wave expansion (PWE) method. The band diagrams show a two frequency band gap for TM polarized modes but no gap for TE modes with this refractive index contrast and relatively small r/a. In the TM band diagram of figure1b the fundamental band gap is centered near a normalized frequency of 0.3. It extends between the normalized frequencies ω_1 =0.2355 (a/λ) and ω_2=0.3532 (a/λ), which corresponds to wavelength range 1.25-1.85µm for the waves with TM polarization.

IOP Conf. Series: Materials Science and Engineering **15** (2010) 012094 doi:10.1088/1757-899X/15/1/012094

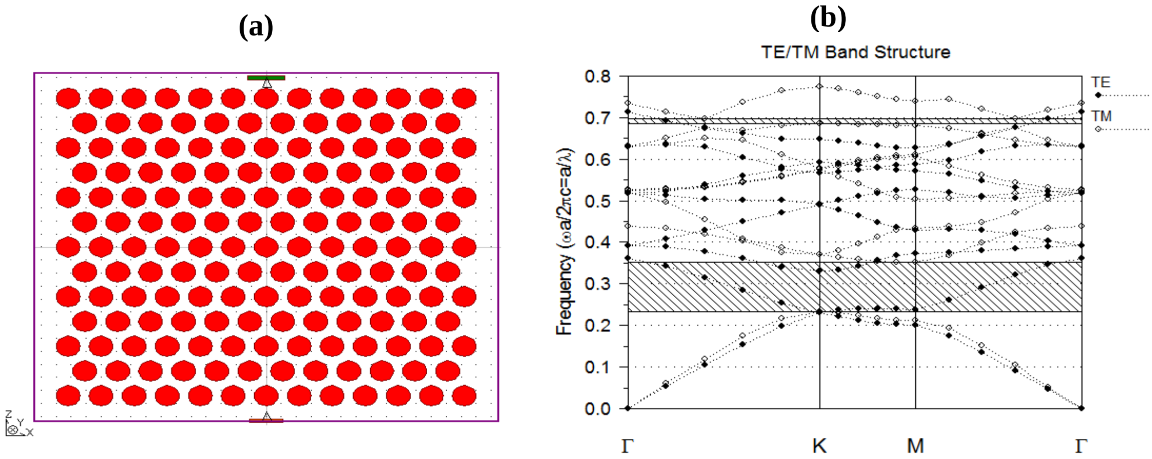

Figure 1. (a) Sight of top of the photonic crystal with a triangular lattice of air holes, with hole radius r=0.36a. **(b)** Dispersions curves and band-gaps for TM and TE polarizations for the 2D lattice without defects.

To study the influence of the polymer on the photonic band gap (PBG), we take the same structure then we filled the air holes (low index) with water (H_2O n=1.33) and polymer (n=1.54) of indium-phosphide-based two dimensional photonic crystal. The fabrication procedure is similar to that described in [22]. A simple filling procedure is described, consisting of infiltration with liquid monomer at room temperature and ambient atmosphere followed by thermal polymerization. The solid state of the infill allows for direct inspection of the infiltrated holes by cross-sectional scanning electron microscopy (SEM). The effect of the filling on the photonic band gap was investigated by optical transmission measurements.

The photonic band gap for the TE and TM polarization of the photonic crystal filled with water and polymer were simulated with 2D plane wave expansion (PWE) method, presented in figure 2a and 2b respectively, shows that the spectral width and position varies with the variation of RI. We can see from figure 2a that there is only one PBG for the TM polarization mode in the frequency range (0.232–0.311) $\omega a/2\pi c$ and a large TM gap appears between the normalized frequencies ω_1 =0.2285 (a/λ) and ω_2=0.29 (a/λ) for air holes filled with polymer, as shown in figure2b.

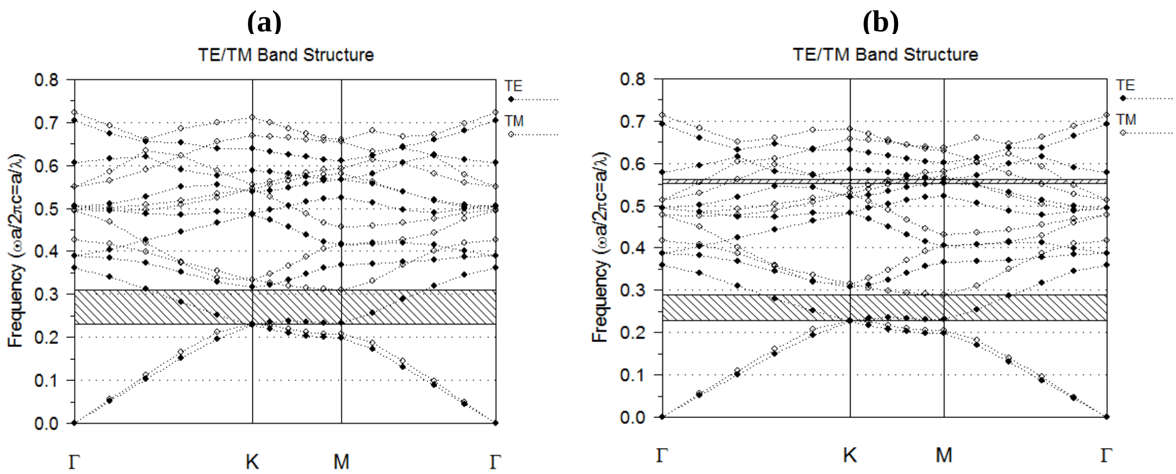

Figure 2. (a) Calculated diagram of photonic band structure for the TE and TM modes of photonic crystal filled with water and **(b)** with polymer.

Further, we simulate PBG for similar PCs, substituting the air in the holes with water and polymer for the TM polarization modes calculation with a 2D finite difference in the time domain (FDTD) simulation method. The computational domain for the FDTD calculation consisted of one lattice unit cell, repeated infinitely by introducing periodic boundary conditions. The lattice unit cell was divided up into 64 × 64 discretization grid points. The convergence and numerical stability and precision of the calculation are tested by increasing the calculation resolution. The transmission spectra for the empty and filled PC are given in figure 3. For the empty structure, the band gap runs from the wavelength λ=1.25 to λ= 1.85µm. At the high-wavelength band edge the transmission rapidly drops by more than three orders of magnitude. The low -wavelength band edge is not as steep as the high-wavelength one, which is attributed to out-of-plane losses. For the filled structure, the air band edge (low wavelength) exhibits a large redshift, while no significant shift is observed for the dielectric band edge (high wavelength). This results from the preferred localization of the light in the low refractive index material for the low-wavelength band [23]. The shift of the air band edge is calculated as a function of the refractive index inside the hole. With this relation, an effective index n_{hole} is obtained from the calculated shift of the air band edge.

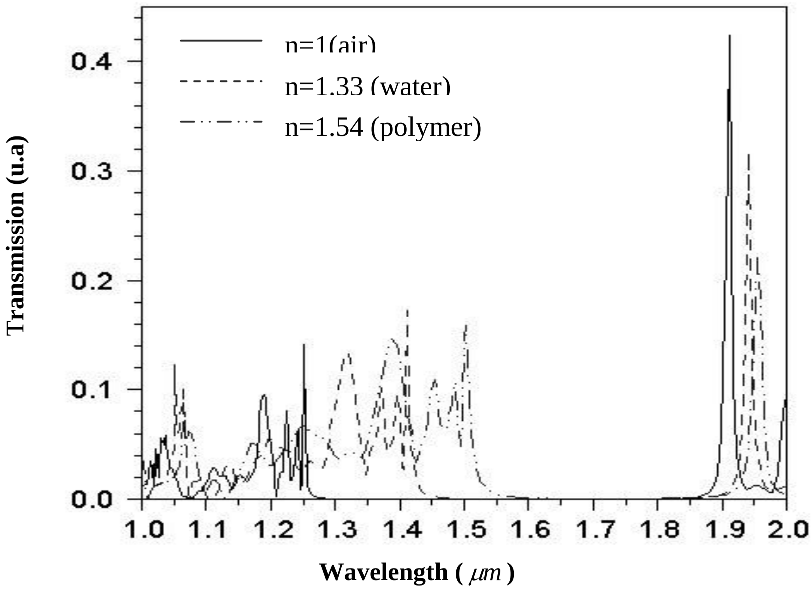

Figure 3. Transmission of the PC with a triangular array of n=1(air), n=1.33 (water) and n=1.54 (polymer).

3. The microcavity design

We consider a finite-sized 13 x13 crystal with a single point defect with no hole missing (H_0). The microcavity is formed by varying the radius of one air hole (see figure 4a). These cavities are chosen because they support different types of modes (monopole, dipole etc.). The detected spectrum has a Lorentzian line shape, and the peak occurs when the PC cavity is at resonance that opens a band pass in the original band gap. The radius of the defect Rc = 0.55a ensures that the cavity can support only one monopole mode excited inside the cavity as shown in figure 4b [24]. The resonance peak at λ=1.71 µm (a/λ= 0.257) was identified as a monopole mode by using 2D finite difference time domain (FDTD) calculations (Full Wave).The quality factor is calculated using the 2D finite-difference time-domain (FDTD) method, combined with fast harmonic analysis. The Q factor is defined as $\lambda_0/\Delta\lambda$, where $\Delta\lambda$ is the full width at half-maximum (FWHM) of the resonator's Lorentzian response and λ_0 is the resonance wavelength. The full width at half-maximum (FWHM) of the single resonance peak yield the cavity quality factor Q=28 325.

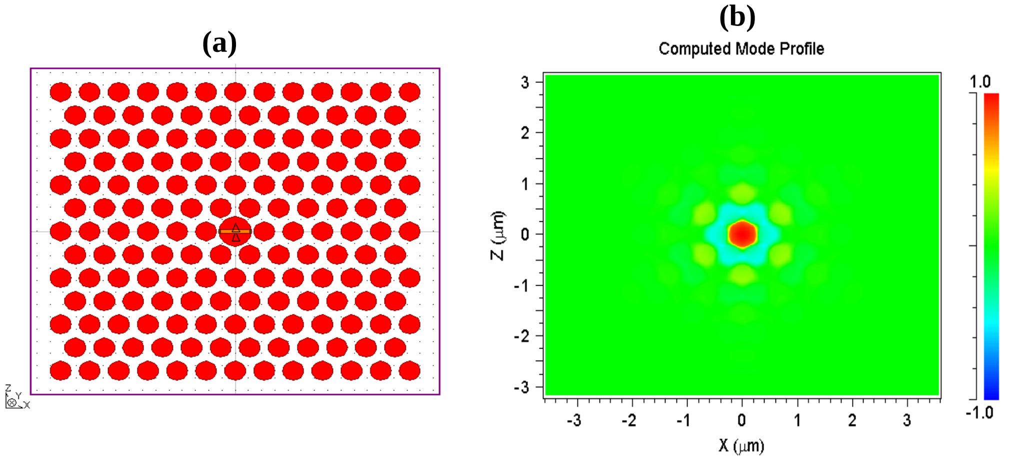

Figure 4. (a) Design of the cavity. The cavity can be formed by varying the radius of the center hole in PC. The radius of the defect can be selected as Rc = 0.55a, **(b)** the intensity field distribution for the cavity at resonant wavelength λ=1.71 μm.

Figure 5 shows TM mode transmission-spectra calculated using 2D Finite-Difference Time-Domain (FDTD) modelling. Spectra are calculated for three homogeneous cover media, air (n= 1), water (n= 1.33) and polymer (n= 1.54). First for filling of PC holes with water (n=1.33), we observe a resonant mode wavelength λ_0=1.8053μm with a quality factor Q=3 965, then for polymer filling of PC holes (n=1.54), the resonant mode shifts towards the wavelength λ_0=1.8582μm and Q=1 373. We clearly observe the resonance peak of this cavity redshift and the resonance quality factor decrease due to the reduced refractive index difference between the holes and the semiconductor membrane, and thus to the reduced reflectivity of the PC boundaries because of the weaker vertical confinement that increases the out-of-plain losses [25].

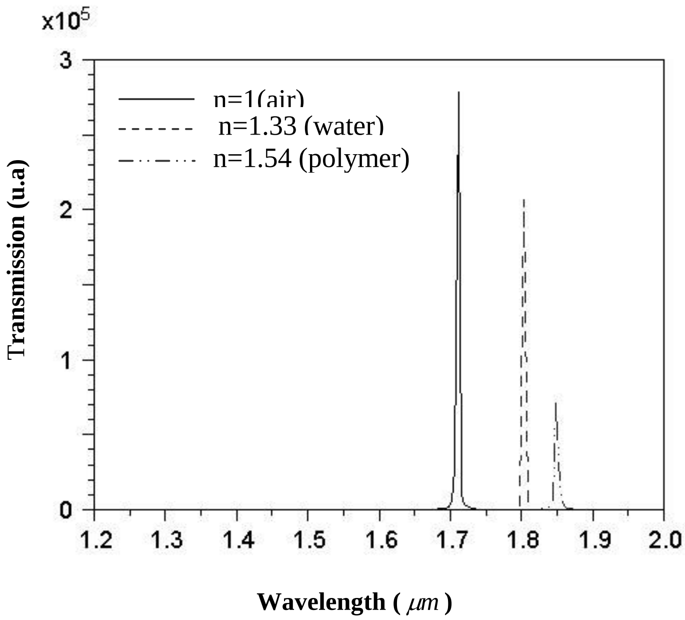

Figure 5. Transmission spectra of the cavity when the RI filled in the air holes of water (n=1.33) and polymer (n=1.54).

4. Local polymer filling of a cavity hole

The same structure is taken again as previously; but in this case the cavity is locally filled with water and polymer (indicated by the darker circle in Figure 6(a)). This procedure has been demonstrated experimentally in [17, 26], a novel lithographic technique of tuning PC devices, based on local mask opening for individual holes. This enables the use of any post production method on the exposed area of the PC, while not affecting other holes in the PC [17].

The transmission characteristics were then simulated with 2D FDTD using perfectly matched layers (PML) as absorbing boundaries. Power monitor was placed inside the microcavity to collect the transmitted spectral power density. Figure 6b shows the 2D FDTD simulation results of the resonant wavelength shift dependence on the refractive index change for three different liquid infiltrations. After pure water is infiltrated, the monopole mode redshifts more than 30 nm due to the increase in the ambient refractive index from 1 to 1.33. The calculated Q factor value for this resonance located at λ=1.74µm was about 20 020. The same calculated is repeated for polymer filling of cavity hole, from the shape of the transmission curves, it can be seen that, the resonant mode shifts towards the wavelength λ_0=1.76073 µm and the quality factor Q=15 211. It is observed that when the cavity is locally infiltrated, the redshift of the resonance peak is of the order of a few manometers and the Q factor decrease slightly. Therefore we have demonstrated the possibility to address differently cavity modes by filling the air holes with different refractive indices.

(a)

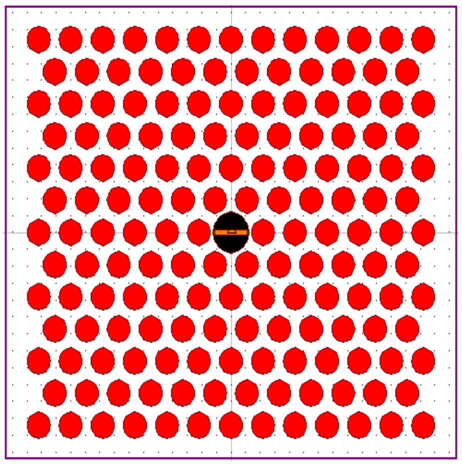

(b)

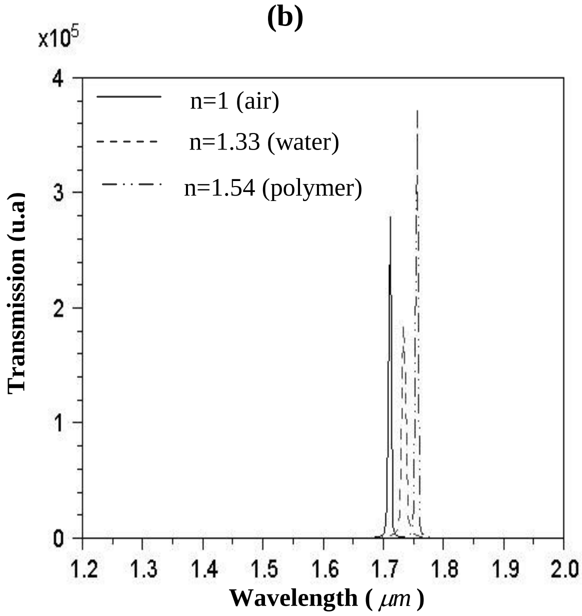

Figure 6. (a) Design of the cavity locally filled with different liquid, **(b)** Transmission spectra of the cavity filled locally in the air hole of two different ambient refractive indices: n=1, n=1.33 and n=1.54.

Since the Q factor can be affected by increasing the size of PC [19], we should select an appropriate crystal size to have the high Q factor and high transmission efficiency. We can see from figure 7(a) that the value of Q factor increases with increasing the PC size and reaches its maximum value at 19x19. We could choose the 19 x19 as the optimum result due to its relatively high Q factor. We saw the Q factor and the transmission efficiency at the resonant mode located at λ_0=1.7609µn are very high (see figure7b), then the calculated Q factor value for this resonance was above 1.0254 10^6. This value compare favourably at those of the previous works [24, 26, 27].

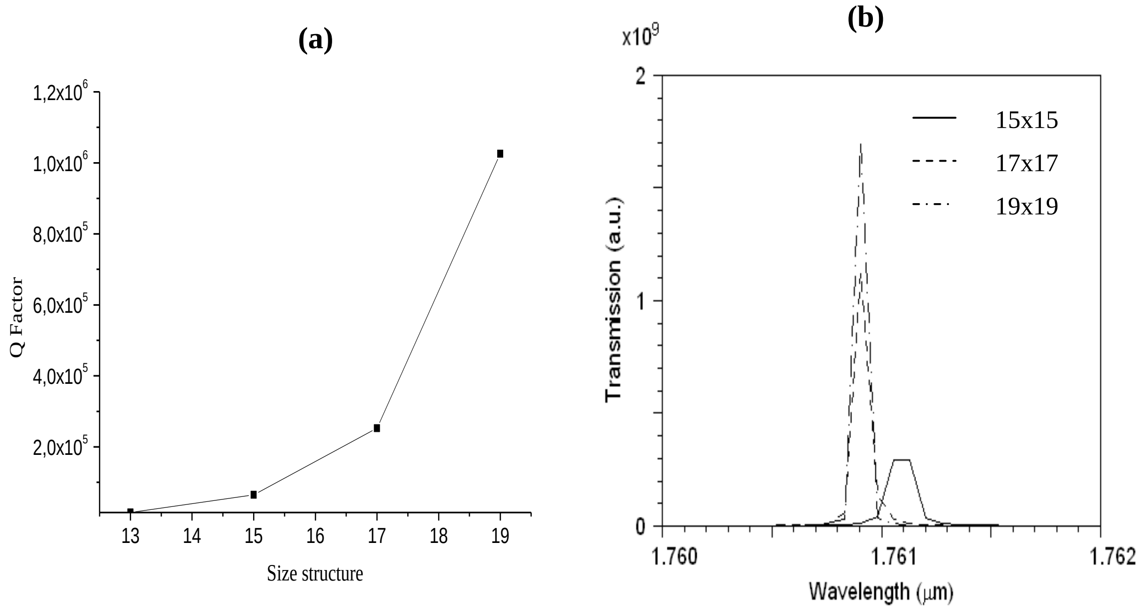

Figure 7. **(a)** The relation of the Q factor of the cavity filled with polymer and the size of photonic crystal. The horizontal abscissa 13, 15, 17, 19 denote the size of the PC is 13x13, 15x15, 17 x17, 19x19, respectively. The 19x19 could be chosen as the optimum result of crystal size. **(b)** Transmission spectrum of the cavity filled locally with polymer (n=1.55) in a finite-sized 15x15 (solid line), 17x17 (dashed line) and 19x19 (dashed-dot line) PC.

5. Conclusion

In summary, we have proposed an ultracompact RI sensor based on microcavity in 2D PC with triangle lattice of air holes. The microcavity is formed by increasing one hole to 0.55a which ensure the cavity can support only one monopole mode. Fist we studied the influence of the polymer on the photonic band gap (PBG), we could show that the optical transmission of a filled photonic crystal structure exhibit a redshift of the air band edge while no significant shift is observed for the dielectric band edge. This study is followed simulation of the microcavity in 2D PC with triangular lattice of air holes filled with polymer; we clearly observe the resonance peak of this cavity redshift and the resonance quality factor decrease. When the cavity is locally filled, the redshift of the resonance peak is of the order of a fewnnanometers. Moreover, the PC size is optimized as 19 x19 air holes to ensure high transmission efficiency and Q factor.

References

[1] J D Joannopoulos, R D Meade and J N Winn 1995 *Princeton University Press, Princeton, NJ.*
[2] E Chomski, G A Ozin 2000 *Adv. Mater.* **12** (14) 1071
[3] C J M. Smith, R M De La Rue, M Rattier, S Olivier, H Benisty, C Weisbush, T F Krauss, R Huodré and U Osterle 2001 *Appl. Phys. Lett.* **78** 1487
[4] J D Joannopoulos, P R Villeneuve and S Fan 1997 *Nature* **386** 143
[5] M De Vittorio, M T Todaro, T Stomeo, R Cingolani, D Cojoc and E Di Fabrizio 2004 *Microelectron. Eng.* **73–74** 388
[6] H Schift, S Park, B Jung, C-G. Choi, C -S Kee, S –P Han, K –B Yoon and J. Gobrecht 2005 *Nanotechnology* **16** S261
[7] K Busch and S John 1999 *Phys. Rev. Lett.* **83** 967
[8] K Yoshino, Y Shimoda, Y Kawagishi, K Nakayama, and M Ozaki 1999 *Appl. Phys.Lett*. **75** 932
[9] E Chow, A Grot, L W Mirkarimi, M Sigalas, and G Girolami 2004 *Opt. Lett.* **29** 1093
[10] M Loncar, A Scherer and Y M Qiu 2003 *Appl. Phys. Lett.* **82** 4648
[11] M Sepulveda, A Call, LM Lechuga, and G Armelles 2006 *Opt. Lett.* **31** 1085-1087
[12] F Intonti, S Vignolini, V Türck, M Colocci, P Bettotti, L Pavesi, S L Schweizer, R. Wehrspohn, and D. Wiersma 2006 *Appl. Phys. Lett*. **89** 211117

[13] A Faraon, D Englund, D Bulla, B Luther-Davies, B J.Eggleton, N Stoltz, P Petroff and J Vučkovic´ 2008 *Appl. Phys. Lett.* **92** 043123
[14] C L C Smith, D K C Wu, M W Lee, C Monat, S Tomljenovic-Hanic, C Grillet, J Eggleton, D Freeman, Y Ruan, S Madden, B Luther-Davies, H Giessen and Y-H Lee 2007 *Appl. Phys. Lett.* **91** 121103
[15] S Tomljenovic-Hanic, C Martijn de Sterke and M J Steel 2006 *Opt. Express* **14** 12451–12456
[16] D Erickson, T Rockwood, T Emery, A Scherer and D. Psaltis 2006 *Opt. Lett.* **31** 59–61
[17] H H J E Kicken, P F A Alkemade, R W van der Heijden, F Karouta, R Notzel, E van der Drift and H W M Salemink 2009 *Opt. Express* **17** 22005-22011
[18] R Ferrini, D Leuenberger, M Mulot, M Qiu, J Moosburger, M Kamp, A Forchel, S Anand and R Houdré 2002 *J. Quantum Elec.* **38** 786
[19] M Qiu and B Jaskorzynska 2003 *Appl. Phys. Lett.* **83** 1074
[20] M Qiu 2002 *Appl. Phys. Lett.* **81** 1163
[21] The FDTD simulations were carried out with Fullwave commercial software by RSoft Design Group, version 6.1, license 16847214
[22] R van der Heijden, C F Carlström, J A P Snijders, R W van der Heijden, F Karouta, R Nötzel, H W M Salemink, B K C Kjellander, C W M Bastiaansen, D J Broer and E van der Drift 2006 *Appl. Phys. Lett.* **88** 161112
[23] S W Leonard, J P Mondia, H M van Driel, O Toader, S John, K Busch, A Birner, U Gösele and V Lehman 2000 *Phys. Rev. B* **61** R2389
[24] X Wang, Z Xu , N Lu 2007 *Opt. Commun*, doi:10.1016/j.optcom.2007.11.040
[25] M Loncar and A Scherer 2004 *in Optical microcavities*, K Vahala ed. (World Scientific Publishing)
[26] P El-Kallassi, S Balog, R Houdré, L Balet, L Li, M Francardi, A Gerardino, A Fiore, R Ferrini and L Zuppiroli 2008 *J.Opt. Soc. Am. B* **25** 1562-1567
[27] M A Dündar, EIs C I Ryckebosch, R Nötzel, F Karouta, Leo J van IJzendoorn and R W van der Heijden 2010 *Opt. Express* **18** 4049-4056